Hindawi
International Journal of Chemical Engineering
Volume 2019, Article ID 8514132, 12 pages
https://doi.org/10.1155/2019/8514132

Research Article

Corrosion Inhibition Mechanism of Mild Steel by Amylose-Acetate/Carboxymethyl Chitosan Composites in Acidic Media

Maria Erna, Herdini Herdini, and Dedi Futra

Department of Chemistry Education, Universitas Riau, Kampus Binawidya KM 12, 5, Pekanbaru 28293, Riau, Indonesia

Correspondence should be addressed to Maria Erna; mariaerna@lecturer.unri.ac.id and Dedi Futra; futra.dedi@yahoo.com

Received 27 August 2018; Revised 3 November 2018; Accepted 7 November 2018; Published 14 February 2019

Academic Editor: Michael Harris

This article details an investigation on the mechanism of corrosion inhibition of mild steel using amylose-acetate-blended carboxymethyl chitosan (AA-CMCh) in acidic media in the context of kinetic and thermodynamic parameters. The surface of mild steel was exposed to test solutions and evaluated using scanning electron microscopy (SEM) and energy dispersive X-ray spectroscopy (EDX). The activation energy (E_a), free energy of adsorption (ΔG), enthalpy of activation (ΔH_{ads}), and entropy of activation (ΔS_{ads}) were determined in order to elucidate the mechanism of corrosion inhibition. The results confirmed that AA could be improved using CMCh as a corrosion inhibitor. The corrosion rate decreased from 1109.00 to 229.70 mdd (79.29%), while corrosion inhibition increased from 35.13 to 89.72%. Sulfate acid (H_2SO_4) of 0.25 M also helped in decreasing the corrosion rate from 2664.4 to 1041.67 mdd (60.9%) while also in increasing corrosion inhibition from 56.94 to 68.31%. The calculated values for ΔG, ΔH_{ads}, and ΔS_{ads} were $-33.22\,kJ{\cdot}mol^{-1}$, $-48.56\,kJ{\cdot}mol^{-1}$, and $0.0495\,kJ{\cdot}mol^{-1}{\cdot}K^{-1}$, respectively. The mechanism of corrosion inhibition of mild steel in the acidic condition is dominated and precipitated by the formation of the Fe-chelate compound, which was confirmed by the SEM/EDS spectrum. The reactions were spontaneous, exothermic, and irregular and takes place on the surface of mild steel.

1. Introduction

Mild steel is widely used for the fabrication of reaction vessels, storage tanks, and petroleum refineries. The usage of corrosive agents in industries, which are detrimental to metals, is unavoidable. To protect metallic surfaces from these agents, various strategies have been proposed and studied, such as cathodic protection, anodic protection, corrosion protection coating, and corrosion inhibitors. The use of inhibitors appears to be the more common due to its low cost, ease-of-procedure, and high efficiency [1, 2]. Many synthetic organics, extracted plants, and inorganic chemicals can be used as inhibitors to prevent mild steel from corroding. Inorganic compounds (e.g., sodium chromate, phosphate, and molybdate) have been proposed as corrosion inhibitors for mild steel in many forms of aqueous media. Karekar et al. [3] reported the use of zinc molybdate nanoparticles as a center nanocontainer for inhibiting the corrosion of mild steel. The zinc molybdate nanoparticles were embedded in a three-layer material consisting of polyaniline, benzotriazole, and polyacrylic acids. The highest corrosion inhibition was reported to be at 5% NaOH and 5% NaCl. However, inorganic compound harms the environment due to its release of toxins and carcinogens to the environment [2].

Extracted plants are widely used as green corrosion inhibitors for mild steel in many acidic media. Abrishami et al. [4] proposed the usage of zinc acetylacetonate-modified *Urtica dioica* leaf extract as an active corrosion inhibitor to protect mild steel in chloride solutions. The proposed corrosion inhibitor reported excellent inhibition efficiency. Krishnan et al. [5] reported the usage of biogenic corrosion inhibition for the protection of mild steel. The biogenic corrosion inhibition based on *Turbinaria ornata* could be

properly utilized as an anti-corrosion agent to reach an inhibition efficiency of 100% at 25 g/L for 5 mins of exposure. Other plants extracted from *Aegle marmelos* fruit [6], *Pongamia pinnata* leaf [7], *Chlorococcum* sp. [8], *Cuscuta reflexa* fruit [9], and *Eriobotrya japonica* Lindl. [10] have been utilized as active corrosion inhibitors for mild steel in many acidic mediums. Corrosion inhibitors based on extracted plants reported inhibition efficiency of >80% [6], >90% for 5 hrs [7], >95% at 11.7 ppm [8], above 95% at 500 ppm [9], and above 95% for 4 hrs [10]. Generally, corrosion inhibition based on green materials performs well in protecting mild steel from corrosion. Green materials contain polar functional groups, i.e., N, S, and O, heterocyclic compound, where its *p*-electrons are responsible for inhibiting corrosion.

Organic chemicals are popularly used as corrosion inhibitors due to the organic compound being easily adsorbed onto metal surfaces. Bouidina et al. [11] analyzed two organic compounds, namely, 1,2-dibenzylidenehydrazine and 1,2-bis(1-phenylethylidene)hydrazine as corrosion inhibitors for mild steel in 1.0 M HCl. The former reported inhibition efficiency that was twice that of the latter, in the range of 26–83%. Chaouiki et al. [12] studied the synthetic organic compounds, i.e., 4-(isopentylamino)-3-nitrobenzonitrile and 3-amino-4-(isopentylamino)benzonitrile for corrosion inhibition of mild steel in a 1.0 M HCl solution and reported that 4-(isopentylamino)-3-nitrobenzonitrile resulted in improvements to inhibition efficiency. Other synthetic organics, such as 1-hydroxyethyl-3-methylimidazolium hexafluorophosphate and 1-hydroxyethyl-3-methylimidazolium bis-(trifluoromethylsulfonyl)imide [13], clopidogrel [14], *p*-vinyl benzene sulfonate and vinyl sulfonate-functionalized polyvinyl alcohol [15], 4-mercaptopyridine-modified sodium dodecyl sulfate [16], 1H-perimidine and 1H-perimidin-2-amine [17], tetrazole derivatives [18], 4-((2,3-dichlorobenzylidene)amino)-3-methyl-1H-1,2,4-triazole-5(4H)-thione [19], 5-aminopyrazole carbonitriles [20], 2-(1-piperidyl)ethyl 3-methyl-4-oxo-2-phenylchromene-8-carboxylate [21], and 1-(2-ami-noethyl)-1-dodecyl-2-(trifluoromethyl)-4,5-dihydro-1H-imidazol-1-ium chloride [22] have been investigated as corrosion inhibitors for the protection of mild steel in HCl, H_2SO_4, and phosphoric acid solution at room temperature. The results confirmed that the compounds reported an inhibition efficiency in the range of 57.1–81.4% [15], 97.0–98.6% [16], 34.6–92.3% [17], 71.1–94.2% [19], 56.8–95.5% [20], 91.2–97.9% [21], and 80.6–99.2% [22]. The high efficiency of these compounds as corrosion inhibitors is due to the polar functions from the presence of S, O, or N atoms, which are used as centers to establish the adsorption process [23, 24].

Chitosan derivatives are currently being touted as a potential material for the protection of metal surfaces from corrosive agents due to their unique structural features, such as rich surface chemistry, biodegradability, bioactivity, biocompatibility, polycationic, and high molecular weight, and the fact that it is renewable [25, 26]. These organic compounds are incubated in acidic mediums at a pH of <6.5, producing a linear poly-base electrolyte with a highly positive charge density. This phenomenon contributed to chitosan and its derivatives becoming highly biocompatible and biodegradable [27]. Many chitosan derivatives have been used to inhibit corrosion in the acidic medium. Cheng et al. [28] reported an anodic corrosion inhibitor based on carboxymethyl chitosan (CMCh) to prevent corrosion on mild steel in an HCl solution. The results confirmed that the CMCh could potentially inhibit corrosion and be used as a control agent to address mild steel corrosion problems. Wan et al. [29] proposed carboxymethyl hydroxypropyl chitosan to inhibit corrosion on the surface of mild steel in a 1.0 M HCl solution. It could also be used as an anticorrosion material at a low concentration to obtain an inhibition efficiency of 95.3% in 1,000 ppm (by weight). Salomon et al. [30] utilized chitosan particle-modified silver nanoparticles to enhance the inhibition of corrosion. This was tested on a St37 steel and 15% H_2SO_4 solution. The corrosion inhibitor based on chitosan-modified silver nanoparticles reported an inhibition efficiency >94%. Alsabagh et al. [31] developed corrosion inhibition based on natural polymer chitosan and used it on carbon steel in a 1.0 M HCl solution. The agent was found to increase the hydrophobic character of chitosan and further enhance its surface-active properties. The results demonstrated that corrosion inhibition was attained at an efficiency of 250 ppm. Umeron et al. [32] proposed another corrosion inhibitor based on natural polymer chitosan to protect the surface of mild steel and reported excellent efficiency (96%) at room temperature. The obtained efficiency in corrosion inhibition was generally due to the specific interaction between functional groups of -COOH and -NH_2 and the metal surface.

This study investigates corrosion inhibition based on amylose acetate-modified carboxymethyl chitosan. The corrosion inhibition efficiency of AA-modified CMCh was used on the surface of mild steel in HCl and H_2SO_4 media. The corrosion inhibitions of AA-modified CMCh on the mild steel surface using kinetic and thermodynamic data were also investigated. The morphological form of the corroding mild steel surface in the presence of AA-modified CMCh was analyzed using scanning electron microscopy (SEM) and energy dispersive X-ray spectroscopy (EDX). The novelty of this work lies in the use of amylose acetate-blended carboxymethyl chitosan as a green corrosion inhibitor for the protection of mild steel in both the HCl and H_2SO_4 solutions. The benefit of this AA-modified CMCh is its high inhibition efficiency (>95%), low inhibitor concentration (in the ppm level), long working period (3 days), and strong bond(s) between the steel and inhibitor solution.

2. Experimental

2.1. Chemicals. All of the chemical used in this work were of analytical grade, and the solutions were prepared using deionized water. Chitosan, carboxymethyl chitosan, dioxane, acetate acid, and silicon carbide sand paper (100, 200, and 400 grades) were purchased from Sigma-Aldrich (St. Louis, USA), while monochloroacetate acid, isopropanol, methanol, ethanol, acetone, chloroform, chloride acid (HCl), and sulfuric acid (H_2SO_4) were purchased from Merck (Darmstadt, Germany). Tapioca tuber and detergent

were procured from the supermarket. The mild steel plate BJTP-24, with an area measuring $2.0 \times 1.0\ cm^2$, used in this work reported a chemical composition of C = 0.16%, Si = 0.19%, Mn = 4.8%, P = 0.16%, S = 0.22%, and balanced Fe.

2.2. Instruments. The FT-IR spectra of amylase acetate were obtained using Spectrum FTIR GX infrared spectrophotometer (PerkinElmer). The surface morphologies of mild steel were imaged using the scanning electron microscope-dispersive X-ray spectrum (SEM-EDS). The pH values of the solutions were measured using a pH meter (Thermo Scientific). The glassware used in this work was cleaned using distilled and deionized waters.

2.3. Amylose Isolation and Surface Modification. The amylose powders were obtained from its cassava base via a simple extraction technique. The preparation of amylose was slightly modified from the one reported in Erna et al. [33]. In brief, the cassava sample was first cleaned using fresh water to remove any soil or contaminant. The cleaned cassava was continuously shredded and directly mixed into fresh water to create a rough pulp. This rough pulp was then shaken and squeezed to obtain a suspension of amylose. The extracted amylose was carefully filtered using gauze to obtain a slurry amylose and carefully rinsed with fresh water several times to get a clean starch. This isolated starch was then air-dried at ambient temperature. The dried starch was thoroughly crushed using a mortar and pestle and immediately purified using a dioxane solution for 4 h to remove any remaining acid(s). Then, the purified starch was again dried at 80°C and carefully dispersed in a solution of *n*-butanol. The obtained amylose was then sterilized using an autoclave for 2 h at a pressure of 15 psi and left to cool at 25°C for 24 hrs. The sterilized amylose was collected via centrifugation (6,500 rpm and 10 min) and washed thoroughly using deionized water and absolute methanol thrice.

To modify the surface of amylose, ~5 g of amylose was immediately acetylated with 25 mL of acetate acid glacial and manually stirred until the solution becomes homogeneous. Then, a mixture consisting of 0.2 mL sulfate acid and 5.0 mL acetate glacial was immediately added into the acetylated amylose and stirred for 1 h at 37°C. A solution of 16.5 mL acetate acid anhydride was carefully added and stirred for another 44 hrs at 37°C. Then, the final acetate-modified amylose was slowly deposited into 200 mL of isopropanol solution and stirred at room temperature. The formed precipitation was then filtered and thoroughly washed with hot distilled water and then air-dried overnight at room temperature. The modified amylose was directly characterized using a spectrum FTIR GX infrared spectrophotometer (PerkinElmer).

2.4. Fabrication of Corrosion Inhibition Based on AA-Blended CMCh. Carboxymethyl chitosan was prepared as per Pang et al. [34]. In brief, ~1.0 g of chitosan powder was mixed with 1.35 g of NaOH and immediately dissolved in 8.0 mL isopropanol containing 2.0 mL of distilled water. The mixture was then kept in a water bath at 60°C. A mixture of 1.5 g of monochloroacetate in 2.0 mL isopropanol was dripped into the chitosan suspension and left for 4 h at ambient temperature. The reaction was stopped via the addition of a solution of 20 mL ethanol (70%). The obtained CMCh was then filtered and washed with ethanol several times, followed by air drying at room temperature.

To make the AA-modified CMCh, a mixture consisting of 200 mg/L CMCh in chloric acid (1.0 M) and 500 mg/L CMCh in sulfate acid (0.25 M) was immediately added into a sample bottle containing 1.0–5.0 mg AA and then carefully stirred until its homogeneous. The CMCh modified with AA was applied on mild steel to analyze the mechanism of corrosion inhibition based on the kinetics and thermodynamics study.

2.5. Preparation of Mild Steel Plates. A mild steel plate was prepared, measuring $1.0 \times 2.0\ cm^2$, and directly cleaned using SiC sand paper (grades 100, 200, and 400). The cleaned mild steel plate was then rinsed with distilled water, acetone, and ethanol several times. It was then immediately dried in an oven for 15 min at 40°C. The dried mild steel was then weighed, and its weight was recorded.

2.6. Determination of Corrosion Rate of Mild Steel in Acidic Media. ~200 mg/L and 500 mg/L of AA-functionalized CMCh were separately added into a solution of 1.0 M HCl and 0.25 M H_2SO_4, respectively. Then, mild steel specimens were directly immersed into HCl and H_2SO_4 media for 3 days and a day, respectively. The steel coupons were carefully rinsed with chloroform and acetone several times. The washed steel coupons were thoroughly brushed and washed with distilled water and ethanol thrice, followed by drying in an oven at 60°C. Then, mild steel specimens were weighed again to compare its respective rates of corrosion. The determination of the corrosion rate of mild steel in acidic media without inhibitors was also conducted for the comparison purposes. The corrosion rate ($g \cdot cm^{-2} \cdot h^{-1}$) was calculated using equation (1), where W_1 and W_2 are the weights of mild steel coupons before and after incubation, respectively, in a test medium. S represents the surface area of corroded steel (dm^2), while t represents the immersion time (h):

$$\text{corrosion rate (CR)} = \frac{W_1 - W_2}{S \cdot t}. \quad (1)$$

2.7. Determination of Inhibition Efficiency, Surface Coverage, and Adsorption-Free Energy Values. The determination of inhibition efficiency was conducted using HCl and H_2SO_4 solutions. A series of AA-functionalized CMCh concentrations, from 200 to 600 mg/L and 500 to 900 mg/L, were thoroughly poured into sample bottles containing HCl and H_2SO_4 solutions, respectively. The prepared steel coupons were then incubated in the HCl and H_2SO_4 solution and carefully rinsed with distilled water, acetone, and ethanol

and then dried in an oven for 15 min at 40°C. The inhibition efficiency (IE%) was calculated using equation (2), while the surface coverage (θ) value was determined using equation (3), where CR_{blank} and CR_{inh} are the values of the corrosion rates of mild steel in the absence and presence of inhibitors, respectively. Meanwhile, the Langmuir isotherm adsorption curve was determined using equation (4), and the free energy of adsorption (ΔG^{o}_{ads}) was investigated using equation (5), where K_{ads} represents the equilibrium constant of the adsorption process and C represents the inhibitor's concentration(s). R represents the gas constant, while T represents the absolute temperature:

$$\mathrm{IE} = \frac{\mathrm{CR}_{\mathrm{blank}} - \mathrm{CR}_{\mathrm{inh}}}{\mathrm{CR}_{\mathrm{blank}}} \times 100, \tag{2}$$

$$\theta = \frac{\mathrm{CR}_{\mathrm{blank}} - \mathrm{CR}_{\mathrm{inh}}}{\mathrm{CR}_{\mathrm{blank}}}, \tag{3}$$

$$K_{\mathrm{ads}} C = \frac{\theta}{1-\theta}, \tag{4}$$

$$\Delta G^{o}_{\mathrm{ads}} = -RT \ln\left(55.5\, K_{\mathrm{ads}}\right). \tag{5}$$

2.8. Determination of Activation of Energy, Enthalpy, and Entropy. The prepared steel coupons have been immersed in HCl and H_2SO_4 solutions containing and not containing inhibitors. Then, the mild steel plates were placed in a thermostat at various temperatures from 28.4 to 60.0°C. The steel plate was rinsed with distilled water, acetone, and ethanol. Afterwards, it was oven-dried for 15 min at 40°C. The activation energy (E_a) was determined using equation (6), where R represents the gas constant, CR represents the corrosion inhibition, K represents the preexponential factor, and T represents the absolute temperature. The values of E_a were calculated from the linear regression between ln CR and $1/T$. The activation enthalpy (ΔH^{o}_{ads}) and entropy (ΔS^{o}_{ads}) can be calculated using equation (7):

$$\mathrm{CR} = k \exp\left(-\frac{E_a}{RT}\right), \tag{6}$$

$$\Delta G^{o}_{\mathrm{ads}} = \Delta H^{o}_{\mathrm{ads}} - T\Delta S^{o}_{\mathrm{ads}}. \tag{7}$$

2.9. Surface Analysis of Mild Steel. The prepared mild steel plates measuring $2.0 \times 1.0\,\mathrm{cm}^2$ were incubated in HCl and H_2SO_4 in the absence/presence of inhibitor under optimum conditions for 3 days. Thereafter, the mild steel specimens were removed, washed with distilled water, degreased with acetone, and then dried at room temperature. The steel specimens were mechanically cut into $1.0\,\mathrm{cm}^2$ chips and then immediately analyzed with SEM and EDX. SEM was performed at a voltage of 5 kV and 5kx magnification on a LEO 1450 VP instrument. The chemical compositions were analyzed using an EDX detector. The attached functional groups on the mild steel surface were investigated using FT-IR spectroscopy equipment (PerkinElmer instrument).

3. Results and Discussion

3.1. Characterization of Amylose-Acetate. The acetate-modified amylose powder for corrosion inhibition is shown in Figure 1. The acetate-functionalized amylose powders are traditionally prepared using the acetylating method. The synthesis of AA involved mixing sulfuric and acetate acids and directly acetylate them via stirring. The powders of acetate functionalized amylose were clearly white. FTIR spectrum of the amylose-acetate is detailed in Figure 2. The O-H stretch peak at $3493.24\,\mathrm{cm}^{-1}$ is from the amylose molecules. The peaks at $1745.65\,\mathrm{cm}^{-1}$ to $1236.42\,\mathrm{cm}^{-1}$ represent a carbonyl (COOH) group of the acetate. These peaks confirmed the occurrence of esterification between amylose and acetate molecules.

3.2. Effect of Inhibitor Concentrations. In order to determine the best condition for the corrosion inhibition response, the inhibitor loading was optimized to include both AA and AA-CMCh. The inhibition efficiency response of corrosion studies based on AA towards mild steel in an acidic medium is shown in Figure 3. In the HCl solution, the inhibition efficiency response gradually increased alongside AA's concentration from 100 to 400 mg/L (Figure 3(a)), while in the H_2SO_4 solution, the inhibition efficiency response also increased alongside AA loading from 100 to 400 mg/L (Figure 3(b)). The increasing inhibition efficiency alongside inhibitor concentration is assumed to be due to the adsorption of inhibitor molecules on the surface of mild steel [35]. With further increase in AA concentration from 400 to 600 ppm in HCl solution and 400 to 500 ppm in H_2SO_4 solution, the responses of inhibition efficiency decreased because the inhibitor has been fully adsorbed onto the mild steel's surface. This confirms that the carboxylic group (COOH) of AA and iron (Fe) of mild steel has bonded. The inhibitor molecules could form a film layer and act as a barrier between mild steel and corrosive media. The optimal AA concentration in HCl and H_2SO_4 solutions, at 400 ppm, was used for further experiments.

The effect of the CMCh : AA ratio towards the inhibition efficiency of mild steel in HCl and H_2SO_4 solution is illustrated in Figure 4. It can be seen that the inhibition efficiency signal increases alongside the CMCh : AA volume loading changed from 1 : 18 to 8 : 4 w/w in the HCl solution (Figure 4(a)). When CMCh : AA changed from 8 : 4 to 9 : 2 w/w, the signal of inhibition efficiency significantly declined. The optimum ratio of CMCh : AA was found at 8 : 4 w/w, with its value of inhibition efficiency at 88.86%. This ratio (8 : 4 w/w) contributed to the interaction energy between the mild steel's surface and thin layer of inhibitor being higher than the interaction energy between the surface of mild steel and water, and consequently, the inhibition efficiency was found to be quite significant.

As can be seen in Figure 4(b), the inhibition efficiency response stabilized when CMCh : AA volume loading changed from 5 : 36 to 30 : 16 w/w in an H_2SO_4 solution. When the ratio of CMCh : AA volume changed from 30 : 16 to 35 : 12 w/w, the inhibition efficiency response increased.

Figure 1: Powder of the amylose functionalized with acetate.

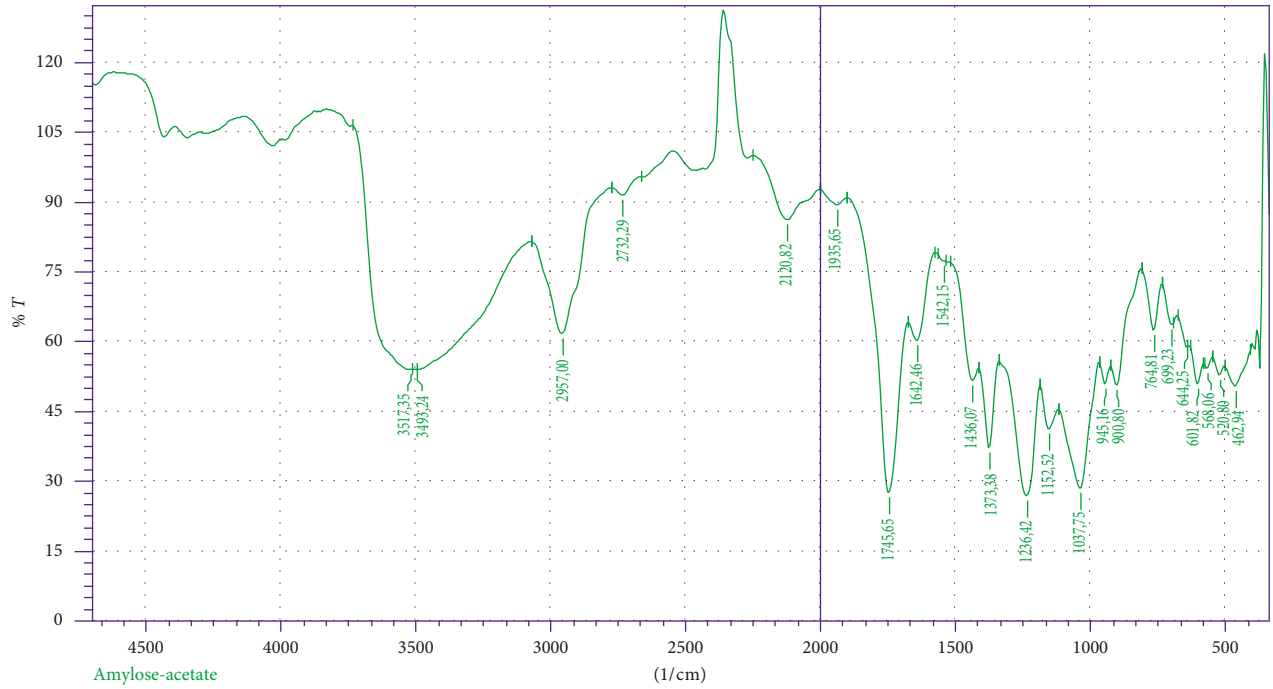

Figure 2: FT-IR spectrum of amylose modified with acetate.

The CMCh : AA volume loading changed again from 35 : 12 to 45 : 4 w/w (Figure 4(b)), and the response of inhibition efficiency gradually reduced in response to this change. This means that the interaction energy between the mild steel's surface and thin layer of the inhibitor took place slowly, with the thin layer of the inhibitor being unable to prevent attacks of the sulfuric ion on the mild steel's surface. This resulted in increased corrosion on the surface [36]. Therefore, the optimum ratio of CMCh : AA in H_2SO_4 solution at 35 : 12 w/w was utilized for the subsequent evaluation of corrosion inhibition.

3.3. Determination of Activation Energy. The activation energy (E_a) of the system in the presence of AA-CMCh was determined using the Arrhenius equation. The Arrhenius plots for mild steel in 1 M HCl with 400 ppm inhibitor is shown in Figure 5. The E_a value determined from the Arrhenius plots in the presence of AA-CMCh was 98.089 kJ·mol^{-1}. This high value of E_a in the presence of an inhibitor was due to the high-energy barrier of the corrosion rate [37], confirming the formation of a complex compound between the inhibitor and Fe ion of mild steel.

3.4. Adsorption Isotherm. The performance of the AA-CMCh as a successful corrosion inhibitor is mainly due to their adsorption ability on the surface of mild steel. This ability has been utilized to determine its mechanism of corrosion inhibition. The Langmuir adsorption isotherm from a plot of C/θ against C at 28°C is shown in Figure 5. The value of the correlation coefficient for AA-CMCh is close to one, which implies that the adsorption of AA-CMCh on the mild steel's surface is well fitted to the Langmuir adsorption isotherm. The calculated K_{ads} and ΔG values are 10496 kJ·mol^{-1} and −33.22 kJ·mol^{-1}, respectively. These values demonstrated that the adsorption types of inhibitors on mild steel surfaces are chemical adsorption. The Langmuir adsorption isotherms from a plot of C/θ against C in 1 M HCl solution at 40°C and 60°C were also plotted (figure not shown). The K_{ads} and ΔG values at 40°C were 7650 kJ·mol^{-1}and −33.722 kJ·mol^{-1}, respectively, while the

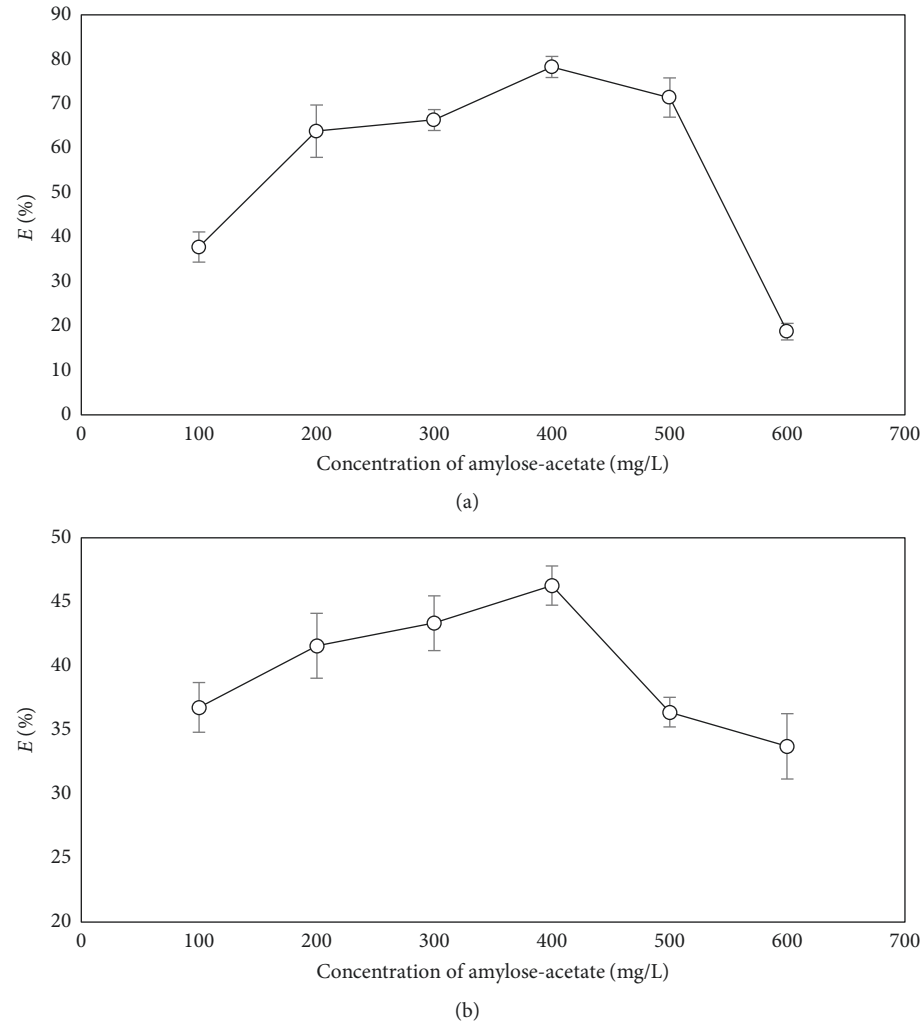

Figure 3: Effect of amylose-acetate concentration on the inhibition efficiency for mild steel in 1.0 M HCl solution (a) and 0.25 M H_2SO_4 solution (b).

K_{ads} and ΔG values at 60°C were found to be 1773 kJ·mol^{-1}and −31.831 kJ·mol^{-1}, respectively. Generally, the obtained values of the ΔG_{ads} were within −33.22 kJ·mol^{-1} to −33.83 kJ·mol^{-1}. The ΔG_{ads} values are ∼−33 kJ·mol^{-1} or more negative, suggesting chemisorption, where charge sharing or charge transfer from an organic compound to the mild steel surface takes place to form a coordinate-type metallic bond [24, 38].

The thermodynamic performance for the corrosion of the mild steel surface in 1 M HCl at multiple concentrations of AA-CMCh composites was obtained from a plot of log(CR/T) versus 1/T and calculated using equation (7). The values of activation enthalpy (ΔH) and activation entropy (ΔS) were −48.56 kJ·mol^{-1} and 0.0495 kJ·mol^{-1}·K^{-1}, respectively. The negative value of ΔH indicates the exothermic nature of the activated-complex formation from the reactants for the rate-determining step of the steel association process. The positive values of ΔS demonstrate irregularity of the adsorbed inhibitors on the mild steel surface [39]. This implies that the activated complex in the rate-determining step represents a dissociation instead of an association process [32].

3.5. Potentiodynamic Polarization Studies. The performance of potentiodynamic polarization for mild steel in an HCl solution (1.0 M) at multiple concentrations of inhibitors at 301 K after 60 min of immersion time is shown in Figure 6. The current anodic and cathodic response decreased as the AA-CMCh loading increased from 100 to 400 ppm due to the large amounts of inhibitor on the electrode's surface and also the moving corrosion potential towards increased negativity. This resulted in the classification of the inhibitor as the mixed type.

The electrochemical parameters, i.e., corrosion potential (E_{corr}), anodic and cathodic Tafel slope (β_c, β_a), corrosion current density (i_{corr}), and inhibition efficiency (IE) obtained from the corresponding polarization curves, are shown in Table 1. In the proposed corrosion inhibitor, the IE (%) was calculated using the following equation:

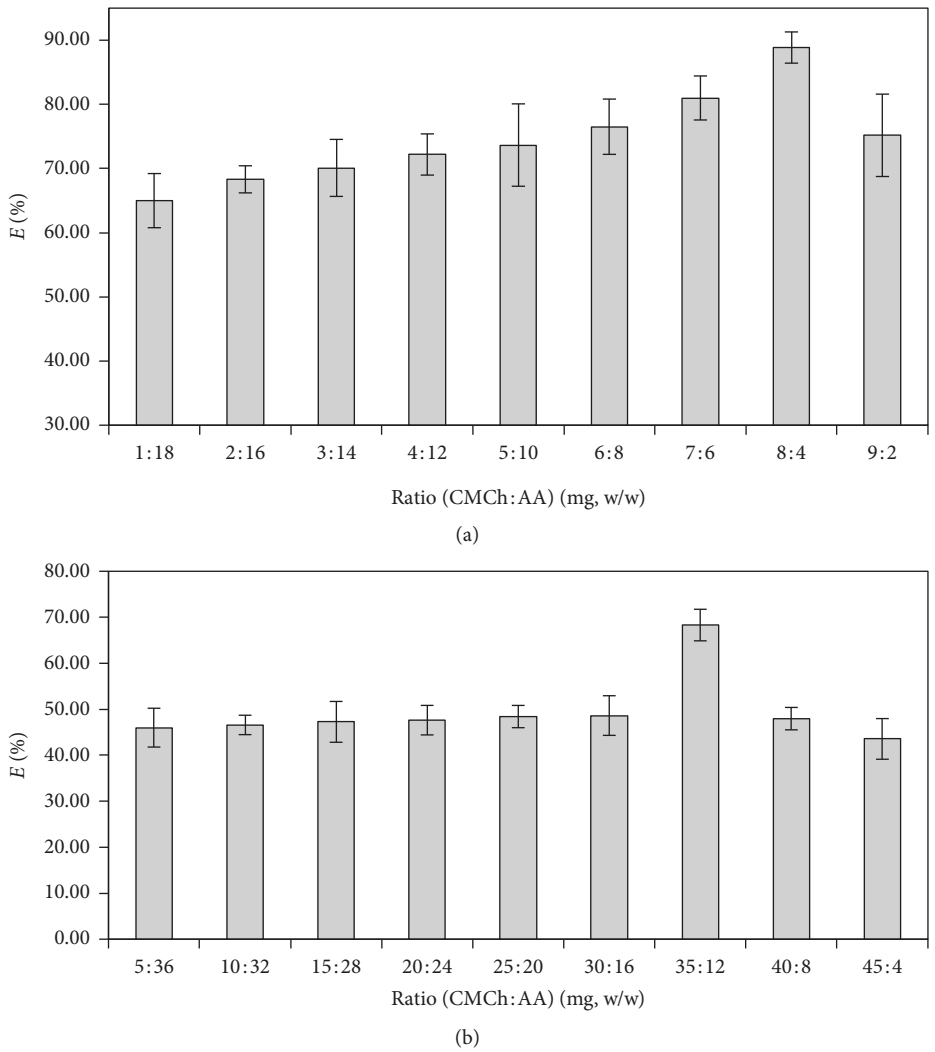

Figure 4: Effect of CMCh : AA concentration on the inhibition efficiency of mild steel in solution of 1.0 M HCl (a) and 0.25 M H_2SO_4 (b) for 3 days.

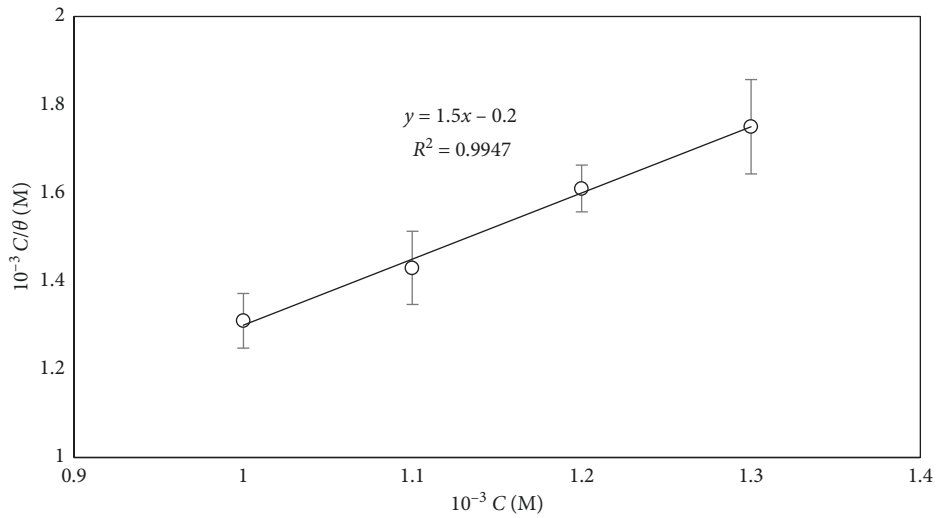

Figure 5: The Langmuir adsorption isotherm curved for mild steel in 1.0 M HCl with 400 ppm of AA-CMCh at 28°C.

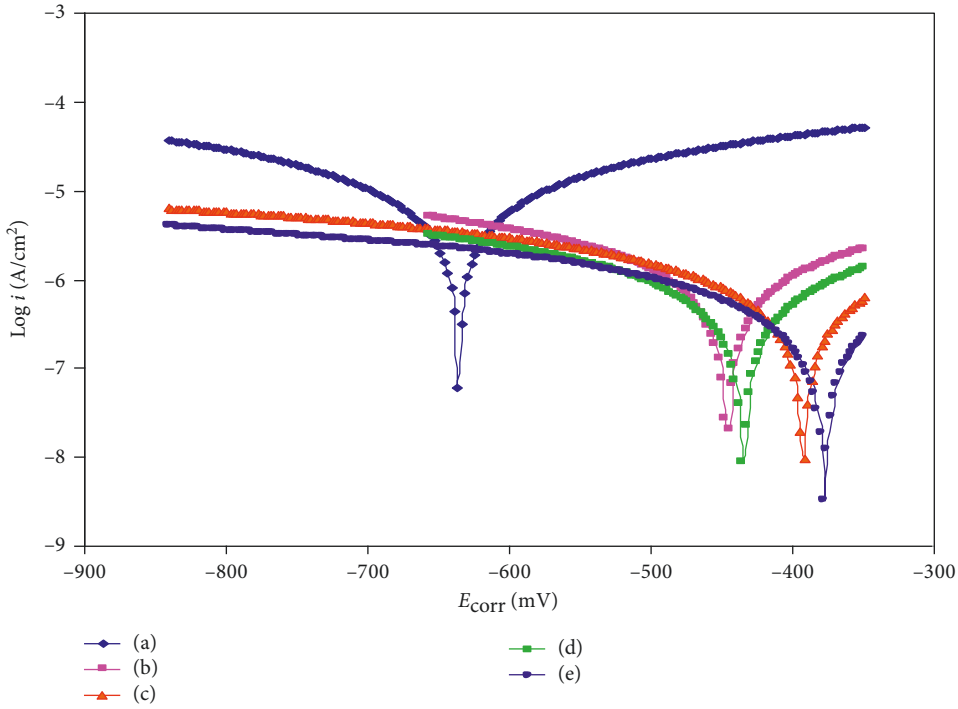

Figure 6: Potentiodynamic polarization curves of mild steel in 1.0 M HCl solution measured in the absence (a) and presence of (b) 100 ppm, (c) 200 ppm, (d) 300 ppm, and (e) 400 ppm of amylose-acetate/carboxymethyl chitosan (AA-CMCh).

Table 1: Electrochemical parameters obtained from polarization measurement in 1.0 M HCl in the presence and absence of a different concentration of AA-CMCh.

AA-CMCh (ppm)	E_{corr} (mV) (Ag/AgCl)	i_{corr} (μA/cm^2)	$ß_c$ (mV/dec)	$ß_a$ (mV/dec)	Inhibition efficiency (%)
0	−641.6	4.30	164.3	164.1	—
100	−448.0	0.52	136.6	144.3	87.94
200	−396.6	0.44	193.8	105.3	89.83
300	−438.4	0.32	142.3	133.8	92.57
400	−381.8	0.10	83.1	53.9	97.65

$$\text{inhibition efficiency } (\%) = \frac{i^0_{corr} - i'_{corr}}{i^0_{corr}} \times 100, \quad (8)$$

where i^0_{corr} and i'_{corr} represent the corrosion current densities without and with the addition of inhibitors, respectively. The results confirmed that the inhibition efficiency response increased, while the corrosion current density decreased when the addition of inhibitors concentration increased. This implies that the inhibitor adsorption on the mild steel's surface and the adsorption process is enhanced and increased inhibition efficiency.

3.6. Surface Characterization: SEM and EDX. In order to determine the effectiveness of the formatted thin layer of the inhibitor on the mild steel's surface, the treated mild steel was imaged using an SEM. SEM images of the mild steel surface in the presence/absence of CMCh in HCl and H_2SO_4 solutions are shown in Figures 7 and 8. In the presence of AA at their respective optimum concentrations (400 ppm) in HCl (Figure 7(a)) and H_2SO_4 solutions (Figure 8(a)), a smooth surface of mild steel can be seen (Figures 7(a) and 8(a)). In the presence of AA-CMCh in HCl (Figure 7(b)) and H_2SO_4 solution (Figure 8(b)), a smoother surface of the mild specimen can be seen (Figures 7(b) and 8(b)). This implies that the AA-CMCh is more effective in inhibiting corrosion on mild steel's surface compared to the AA inhibitor. This feature probably contributed to the homogeneity and biocompatibility of the AA-CMCh composites on the mild steel's surface. Generally, a smoother surface of the mild steel specimen denote that the AA-CMCh has adsorbed onto the mild steel's surface and protected specimens from direct acid attacks.

The EDX spectra of the mild steel and control specimen in HCl solution is shown in Figure 9. The surface of mild steels as a control specimen before treatment (Figure 9(c)) and the presence of AA-CMCh (Figure 9(b)) exhibit a smooth and uniform surface. The morphology in the presence AA was slightly damaged and rough (Figure 9(a)). This confirmed that the mild steel surface is well protected from acidic attacks and prevented from corroding. Table 2 shows the percentage of atomic contents in the inhibitor and control specimens. The EDX spectrum in the presence of AA-CMCh confirmed that the concentration of the Cl ion is

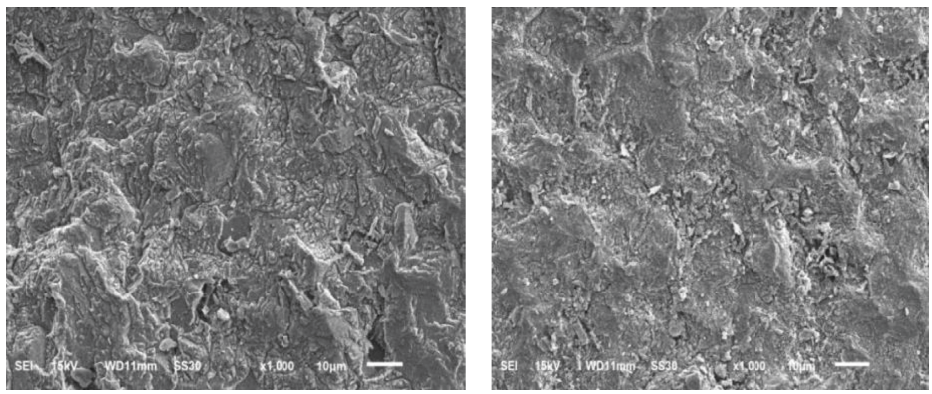

(a) (b)

Figure 7: SEM images of mild steel surfaces in 1 M HCl with AA (a) and AA-CMCh (b).

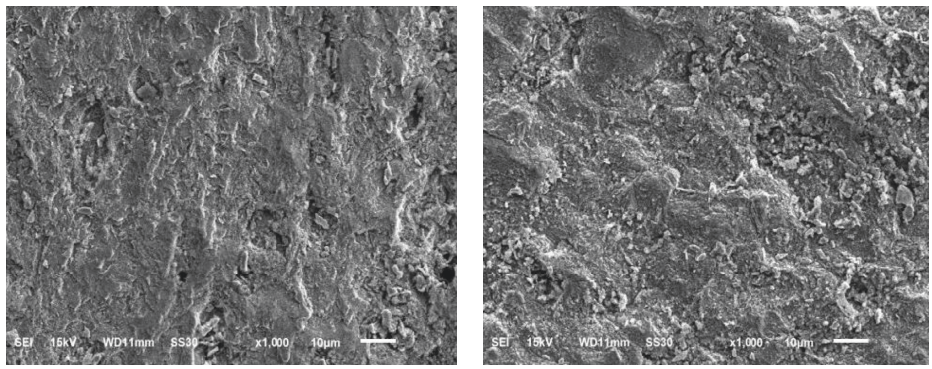

(a) (b)

Figure 8: SEM micrographs of the mild steel surface in 0.25 M H_2SO_4 with AA (a) and AA-CMCh (b).

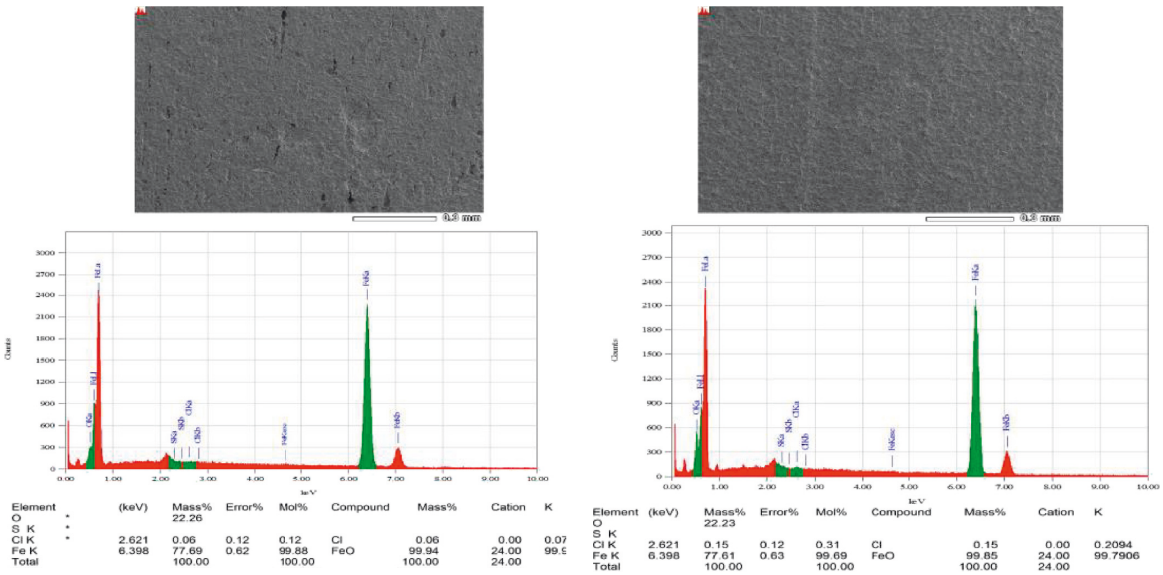

(a) (b)

Figure 9: Continued.

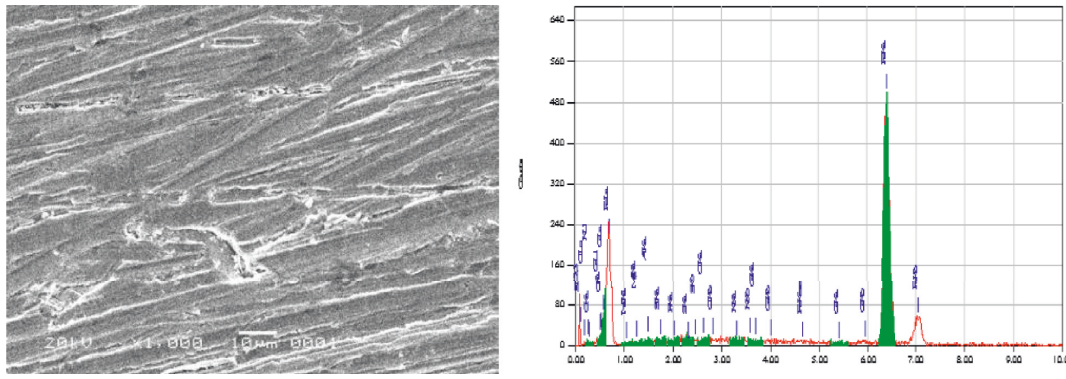

(c)

Figure 9: SEM/EDX spectra of the mild steel surface in 1 M HCl: (a) AA; (b) AA-CMCh blended; (c) control.

Table 2: Percentage atomic contents of elements measured using the EDX technique.

Inhibitors	Fe	O	S	Cl	C
Control	96.64	1.97	—	0.12	0.27
AA	77.69	22.26	—	0.06	13.46
AA-CMCh	77.61	22.23	—	0.15	16.49

higher than that of the presence of AA, whilst the concentration of C in the control specimen prior to treatment was lower than that of the treated specimen due to the inhibitor absorbed onto the mild steel's surface. The concentration of Fe and O from the inhibitor of AA is not significantly different than the inhibitor of AA-CMCh (Table 2). Generally, both AA and AA-CMCh inhibitors are able to inhibit the mild steel specimen from a direct attack by the Cl ion, which protects the mild steel surface from an aggressive environment.

3.7. Mechanism of Inhibition. The adsorption of AA-blended CMCh on mild steel can be clearly defined by considering the chemisorption processes. The specific mechanism of corrosion inhibition of AA-CMCh to the surface of mild steel coupons is detailed in the following equations:

$$\mathrm{Fe} + \text{AA-CMCh} \longleftrightarrow \mathrm{Fe(AA\text{-}CMCh)_{ads}} \quad (9)$$

$$\mathrm{Fe(AA\text{-}CMCh)_{ads}} \longleftrightarrow \mathrm{Fe^{2+}} + \text{AA-CMCh} + ne^{-} \quad (10)$$

$$\text{AA-CMCh}_{aq} + \mathrm{H_2O_{ads}} \longleftrightarrow \text{AA-CMCh}_{ads} + \mathrm{H_2O_{aq}} \quad (11)$$

The chemisorption of AA-CMCh on mild steel is denoted by the donor-acceptor interactions between the lone pair of the electron from the carbonyl and amine groups of AA-CMCh with the d-orbitals of Fe. The value of free energy from the AA-CMCh adsorption was $-33\ \mathrm{kJ{\cdot}mol^{-1}}$ or more negative. This confirms that the adsorption mechanism of the AA-CMCh on the surface of the mild steel coupon was chemically adsorbed. The inhibition of corrosion begins by the displacement of water molecules by the inhibitor's capacity toward specific adsorption of the inhibitor on the metal's surface [40].

4. Conclusions

The corrosion inhibition mechanism based on carboxymethyl chitosan/amylose-acetate composites used to protect mild steel in an acidic medium was successfully investigated. The AA-CMCh base inhibitor showed excellent inhibition performance in the case of mild steel in a 1 M HCl solution. The inhibiting efficiencies decreased in the order of AA-CMCh > AA. The inhibitor adsorptions on the mild steel's surface are chemically adsorbed, while the corrosion inhibition mechanism on the mild steel's surface was spontaneous, exothermal, and irregular and took place due to the formation of the Fe-chelate compound on the surface of the mild steel specimen. The adsorption of the inhibitors on the mild steel specimen in acidic media solution comports with that of the Langmuir adsorption isotherm. The negative values of the ΔG_{ads} and ΔH indicated that the adsorption reaction took place spontaneously and exothermally.

Data Availability

The data used to support the findings of this study are available from the corresponding author upon request.

Conflicts of Interest

The authors declare that there are no conflicts of interest regarding the publication of this work.

Acknowledgments

The authors gratefully acknowledge financial support from the Directorate General of Higher Education of Ministry (DIKTI), the Ministry of Research, Technology and Higher Education, through a fundamental grant of the Universitas Riau, Indonesia.

References

[1] B. Xu, W. Yang, Y. Liu, X. Yin, W. Gong, and Y. Chen, "Experimental and theoretical evaluation of two pyridinecarboxaldehyde thiosemicarbazone compounds as corrosion inhibitors for mild steel in hydrochloric acid solution," *Corrosion Science*, vol. 78, pp. 260–268, 2014.

[2] S. A. Umoren and U. M. Eduok, "Application of carbohydrate polymers as corrosion inhibitors for metal substrates in different media: a review," *Carbohydrate Polymers*, vol. 140, pp. 314–341, 2016.

[3] S. E. Karekar, U. D. Bagale, S. H. Sonawane, B. A. Bhanvase, and D. V. Pinjari, "A smart coating established with encapsulation of Zinc Molybdate centred nanocontainer for active corrosion protection of mild steel: release kinetics of corrosion inhibitor," *Composite Interfaces*, vol. 25, no. 9, pp. 785–808, 2018.

[4] S. Abrishami, R. Naderi, and B. Ramezanzadeh, "Fabrication and characterization of zinc acetylacetonate/*Urtica dioica* leaves extract complex as an effective organic/inorganic hybrid corrosion inhibitive pigment for mild steel protection in chloride solution," *Applied Surface Science*, vol. 457, pp. 487–496, 2018.

[5] M. Krishnan, H. Subramanian, H.-U. Dahms et al., "Biogenic corrosion inhibitor on mild steel protection in concentrated HCl medium," *Scientific Report*, vol. 8, p. 2609, 2018.

[6] N. Bhardwaj, D. Prasad, and R. Haldhar, "Study of the *Aegle marmelos* as a green corrosion inhibitor for mild steel in acidic medium: experimental and theoretical approach," *Journal of Bio- and Tribo-Corrosion*, vol. 4, no. 4, p. 61, 2018.

[7] T. K. Bhuvaneswari, V. S. Vasantha, and C. Jeyaprabha, "*Pongamia pinnata* as a green corrosion inhibitor for mild steel in 1N sulfuric acid medium," *Silicon*, vol. 10, no. 5, pp. 1793–1807, 2018.

[8] M. P. Rai, A. Khanra, S. Rai, M. Srivastava, and R. Prakash, "Pivotal role of levoglucosenone and hexadecanoic acid from microalgae *Chlorococcum* sp. for corrosion resistance on mild steel: electrochemical, microstructural and theoretical analysis," *Journal of Molecular Liquids*, vol. 266, pp. 279–290, 2018.

[9] A. Saxena, D. Prasad, and R. Haldhar, "Investigation of corrosion inhibition effect and adsorption activities of *Cuscuta reflexa* extract for mild steel in 0.5 M H_2SO_4," *Bioelectrochemistry*, vol. 124, pp. 156–164, 2018.

[10] X. Zheng, M. Gong, Q. Li, and L. Guo, "Corrosion inhibition of mild steel in sulfuric acid solution by loquat (*Eriobotrya japonica* Lindl.) leaves extract," *Scientific Report*, vol. 8, p. 9140, 2018.

[11] A. Bouoidina, F. El-Hajjaji, M. Drissi et al., "Towards a deeper understanding of the anticorrosive properties of hydrazine derivatives in acid medium: experimental, DFT and MD simulation assessment," *Metallurgical and Materials Transactions A*, vol. 49, no. 10, pp. 5180–5191, 2018.

[12] A. Chaouiki, H. Lgaz, I.-M. Chung et al., "Understanding corrosion inhibition of mild steel in acid medium by new benzonitriles: insights from experimental and computational studies," *Journal of Molecular Liquids*, vol. 266, pp. 603–616, 2018.

[13] Y. Guo, Z. Chen, Y. Zuo, Y. Chen, W. Yang, and B. Xu, "Ionic liquids with two typical hydrophobic anions as acidic corrosion inhibitors," *Journal of Molecular Liquids*, vol. 269, pp. 886–895, 2018.

[14] E. Naseri, M. Hajisafari, A. Kosari, M. Talari, S. Hosseinpour, and A. Davoodi, "Inhibitive effect of Clopidogrel as a green corrosion inhibitor for mild steel; statistical modeling and quantum Monte Carlo simulation studies," *Journal of Molecular Liquids*, vol. 269, pp. 193–202, 2018.

[15] R. Geethanjali and S. Subhashini, "Synthesis and kinetics of corrosion inhibition of water-soluble terpolymer of polyvinyl alcohol functionalized with vinyl sulfonate and *p*-vinyl benzene sulfonate, in molar HCl," *Journal of Bio- and Tribo-Corrosion*, vol. 4, no. 4, p. 60, 2018.

[16] P. Han, W. Li, H. Tian et al., "Designing and fabricating of time-depend self-strengthening inhibitor film: synergistic inhibition of sodium dodecyl sulfate and 4-mercaptopyridine for mild steel," *Journal of Molecular Liquids*, vol. 268, pp. 425–437, 2018.

[17] X. He, J. Mao, Q. Ma, and Y. Tang, "Corrosion inhibition of perimidine derivatives for mild steel in acidic media: electrochemical and computational studies," *Journal of Molecular Liquids*, vol. 269, pp. 260–268, 2018.

[18] A. A. Mahmmod, I. A. Kazarinov, A. A. Khadom, and H. B. Mahood, "Experimental and theoretical studies of mild steel corrosion inhibition in phosphoric acid using tetrazoles derivatives," *Journal of Bio- and Tribo-Corrosion*, vol. 4, no. 4, p. 58, 2018.

[19] M. Messali, M. Larouj, H. Lgaz et al., "A new schiff base derivative as an effective corrosion inhibitor for mild steel in acidic media: experimental and computer simulations studies," *Journal of Molecular Structure*, vol. 1168, pp. 39–48, 2018.

[20] A. Mishra, C. Verma, S. Chauhan et al., "Characterization, and corrosion inhibition performance of 5-aminopyrazole carbonitriles towards mild steel acidic corrosion," *Journal of Bio- and Tribo-Corrosion*, vol. 4, p. 53, 2018.

[21] N. Saini, R. Kumar, H. Lgaz et al., "Minified dose of urispas drug as better corrosion constraint for soft steel in sulphuric acid solution," *Journal of Molecular Liquids*, vol. 269, pp. 371–380, 2018.

[22] K. Zhang, W. Yang, Y. Chen et al., "Enhanced inhibitive performance of fluoro-substituted imidazolium-based ionic liquid for mild steel corrosion in hydrochloric acid at elevated temperature," *Journal of Materials Science*, vol. 53, no. 20, pp. 14666–14680, 2018.

[23] K. R. Ansari, M. A. Quraishi, and A. Singh, "Corrosion inhibition of mild steel in hydrochloric acid by some pyridine derivatives: an experimental and quantum chemical study," *Journal of Industrial and Engineering Chemistry*, vol. 25, pp. 89–98, 2015.

[24] L. O. Olasunkanmi, I. B. Obot, M. M. Kabanda, and E. E. Ebenso, "Some quinoxalin-6-yl derivatives as corrosion inhibitors for mild steel in hydrochloric acid: experimental and theoretical studies," *Journal of Physical Chemistry C*, vol. 119, no. 28, pp. 16004–16019, 2015.

[25] M. Ewis, S. S. Elkholy, and M. Z. Esabee, "Antifungal efficacy of chitosan and its thiourea derivatives upon the growth of some sugar-beet pathogens," *International Journal of Biological Macromolecules*, vol. 38, no. 1, pp. 1–8, 2006.

[26] Z.-X. Tang, J.-Q. Qian, and L.-E. Shi, "Characterizations of immobilized neutral lipase on chitosan nano-particles," *Materials Letters*, vol. 61, no. 1, pp. 37–40, 2007.

[27] M. N. El-Haddad, "Chitosan as a green inhibitor for copper corrosion in acidic medium," *International Journal of Biological Macromolecules*, vol. 55, pp. 142–149, 2013.

[28] S. Cheng, S. Chen, T. Liu, X. Chang, and Y. Yin, "Carboxymenthylchitosan as an ecofriendly inhibitor for mild steel in 1 M HCl," *Materials Letters*, vol. 61, no. 14-15, pp. 3276–3280, 2007.

[29] K. Wan, P. Feng, B. Hou, and Y. Li, "Enhanced corrosion inhibition properties of carboxymethyl hydroxypropyl chitosan for mild steel in 1.0 M HCl solution," *RSC Advances*, vol. 6, no. 81, pp. 77515–77524, 2016.

[30] M. M. Solomon, H. Gerengi, T. Kaya, and S. A. Umoren, "Enhanced corrosion inhibition effect of chitosan for St37 in 15% H_2SO_4 environment by silver nanoparticles," *International Journal of Biological Macromolecules*, vol. 104, pp. 638–649, 2017.

[31] A. M. Alsabagh, M. Z. Elsabee, Y. M. Moustafa, A. Elfky, and R. E. Morsi, "Corrosion inhibition efficiency of some hydrophobically modified chitosan surfactants in relation to their surface active properties," *Egyptian Journal of Petroleum*, vol. 23, no. 4, pp. 349–359, 2014.

[32] S. A. Umoren, M. J. Banera, T. Alonso-Garcia, C. A. Gervasi, and M. V. Mirífico, "Inhibition of mild steel corrosion in HCl solution using chitosan," *Cellulose*, vol. 20, no. 5, pp. 2529–2545, 2013.

[33] M. Erna, Y. Eryanti, and A. Dahliaty, "Modifikasi amilosa dari pati tapioka dan garut menjadi amilosa asetat," *Jurnal Pilar Sains*, vol. 7, pp. 28–30, 2008.

[34] H. T. Pang, X. G. Chen, H. J. Park, D. S. Cha, and J. F. Kennedy, "Preparation and rheological properties of deoxycholate-chitosan and carboxymethyl-chitosan in aqueous systems," *Carbohydrate Polymers*, vol. 69, no. 3, pp. 419–425, 2007.

[35] K. K. Anupama and J. Abraham, "Electroanalytical studies on the corrosion inhibition behavior of guava (*Psidium guajava*) leaves extract on mild steel in hydrochloric acid," *Research on Chemical Intermediates*, vol. 39, no. 9, pp. 4067–4080, 2012.

[36] M. E. Al-Dokheily, H. M. Kredy, and R. N. Al-Jabery, "Inhibition of copper corrosion in H_2SO_4, NaCl and NaOH solutions by *Citrullus colocynthis* fruits extract," *Journal of Natural Sciences Research*, vol. 4, pp. 60–73, 2014.

[37] M. H. Hussin and M. J. Kassim, "The corrosion inhibition and adsorption behavior of *Uncaria gambir* extract on mild steel in 1M HCl," *Materials Chemistry and Physics*, vol. 125, no. 3, pp. 461–468, 2011.

[38] K. R. Ansari, M. A. Quraishi, and A. Singh, "Isatin derivatives as a non-toxic corrosion inhibitor for mild steel in 20% H_2SO_4," *Corrosion Science*, vol. 95, pp. 62–70, 2015.

[39] B. Zerga, A. Attayibat, M. Sfaira et al., "Effect of some tripodal bipyrazolic compounds on C38 steel corrosion in hydrochloric acid solution," *Journal of Applied Electrochemistry*, vol. 40, no. 9, pp. 1575–1582, 2010.

[40] H. Ashassi-Sorkhabi and S. A. Nabavi-Amri, "Corrosion inhibition of carbon steel in petroleum/water mixtures by n-containing compounds," *Acta Chimica Slovenica*, vol. 47, pp. 507–517, 2000.